HUMAN GENE THERAPY 22:1537–1550 (December 2011)

DOI: 10.1089/hum.2011.076

Sonoporation Delivery of Interleukin-27 Gene Therapy Efficiently Reduces Prostate Tumor Cell Growth *In Vivo*

Olga Zolochevska,[1] Xueqing Xia,[2] B. Jill Williams,[3] Alistair Ramsay,[4] Shulin Li,[2] and Marxa L. Figueiredo[1,5]

Abstract

We have examined the potential of a novel cytokine, interleukin-27 (IL-27), for gene therapy of prostate cancer. IL-27 is the most recently characterized member of the family of heterodimeric IL-12-related cytokines and has shown promise in halting tumor growth and mediating tumor regression in several cancer models. In the present study, we examined the efficacy of a new mode of gene delivery to prostate tumors: low-frequency ultrasound irradiation or "sonoporation." We also examined the potential of IL-27 gene delivery by sonoporation to treat and reduce the growth of prostate cancer *in vivo*. We used three models of immune-competent prostate adenocarcinoma and characterized the tumor-growth reduction, gene-profile expression, and effector cellular profiles. Our results suggest that IL-27 can be effective in reducing tumor growth and can help enhance accumulation of effector cells in prostate tumors *in vivo*. These results are promising, because they are potentially relevant to developing novel therapies that can be translated by using the novel and effective sonoporation gene-therapy delivery strategy.

Introduction

Heterogeneity of prostate cancer has culminated in an inadequacy of single-treatment regimens and inefficient patient management. An urgent need has emerged for new therapies that can be administered into the primary tumor with systemic effects and without toxicity. Also, an important current area of research is the design and investigation of new agents and their preclinical screening in clinically relevant *in vivo* models (*i.e.*, immune-competent models). Immune-stimulatory strategies have the potential to combat cancer and generate long-term antitumor effects. Several clinical and preclinical studies point to the promise of using cytokines alone or in combination with cytotoxic gene therapy or radiation to achieve stimulation of systemic immune cellular responses (Freeman *et al.*, 1997; Toda *et al.*, 2001; Nakamori *et al.*, 2002; Hwang *et al.*, 2005; Fujita *et al.*, 2006). Despite promising clinical results, however, the data suggest that the efficacy of immune-stimulatory treatments needs to be improved. We propose the use of a novel cytokine, interleukin-27 (IL-27), for the treatment of prostate cancer. IL-27 is the most recently characterized member of the family of heterodimeric IL-12-related cytokines. IL-27 has shown promise in halting tumor growth and mediating tumor regression in several cancer models, including primary neuroblastoma (Salcedo *et al.*, 2004) and colorectal (Engel and Neurath, 2010) and breast (Zhu *et al.*, 2010) carcinomas. IL-27 is a heterodimeric cytokine composed of p28, an IL-12p35-related protein, and Epstein-Barr virus–induced gene 3 (EBI3), an IL-12p40-related protein. IL-27 is produced primarily from activated dendritic cells and induces proliferation of naive but not memory $CD4^+$ T cells (Pflanz *et al.*, 2002). It also synergizes with IL-12 in interferon-γ (IFNγ) production from naive T and natural killer (NK) cells. WSX1/TCCR, one of the IL-27 receptor molecules, is highly expressed in lymphoid organs, particularly in naive $CD4^+$ T and NK cells. The IL-27/WSX1 signaling induces T-bet and IL-12 receptor (IL-12R) β2 expression, and thus IL-27 plays a crucial role in the initiation of Th1 differentiation before the IL-12/IL-12R system (Lucas *et al.*, 2003; Takeda *et al.*, 2003).

In the present study, we had two broad goals. First, we examined the efficacy of a new mode of gene delivery to prostate tumors: low-frequency ultrasound (US) irradiation or "sonoporation." Over the past number of years, several

[1]Department of Pharmacology and Toxicology, University of Texas Medical Branch, Galveston, TX 77555.
[2]Department of Pediatrics, University of Texas M.D. Anderson Cancer Center, Houston, TX 77030.
[3]Department of Urology, Louisiana State University Health Sciences Center, Shreveport, LA 71103.
[4]Louisiana Vaccine Center, and Department of Microbiology, Immunology and Parasitology, Louisiana State University Health Sciences Center, New Orleans, LA 70112.
[5]Department of Comparative Biomedical Sciences, Louisiana State University, Baton Rouge, LA 70803.

reports have described the combined use of sonoporation and microbubbles to achieve delivery of naked plasmid DNA-encoded transgenes into cancer cells in tissue culture–based systems (Escoffre *et al.*, 2011). In particular, sonoporation has been shown to be as effective in facilitating gene transfer into selected cancer cell lines as either electroporation or liposome-based gene-transfer systems (Feril *et al.*, 2006). Sonoporation is an emerging and promising physical method for cancer gene therapy that typically operates in the range of 35 KHz to 1 MHz and has several advantages over other nonphysical means of nucleic acid delivery, including the ability to also deliver drugs or small molecules. To further improve the efficiency of sonoporation, promising studies include mixing DNA, siRNA, small molecules, or viral vectors with gas-filled lipid molecules called microbubbles (MB). MB are gas–liquid emulsions consisting of a gaseous core surrounded by a shell and are usually 1–7 μm in size. MB traditionally have been developed as contrast agents for enhancing clinical US imaging (Deshpande *et al.*, 2010). However, MB now have an increasingly significant role in both diagnostic and therapeutic applications of US. The motion of MB disruption increases the permeability of cell membranes, enhancing therapeutic uptake, and can locally increase drug/nucleic acid transport across solid tumors (Stride and Coussios, 2010). For nucleic acid delivery, sonoporation in the presence of MB has been shown to increase plasmid transfection efficiency *in vitro* by several orders of magnitude. The formation of short-lived pores in the plasma membrane up to $\sim$100 nm in diameter lasts a few seconds, and is implicated as the dominant mechanism associated with acoustic cavitation (Newman and Bettinger, 2007).

Transgene expression has been shown to be $\sim$19-fold higher than gene expression facilitated by electroporation, with similar modest effects on cell viability, a finding also supported by a recent review (Wells, 2010). We have confirmed that a sonoporation strategy is effective in delivering plasmid DNA mixed with SonoVue MB to prostate tumors of both mouse and human origin *in vivo*. We also examined the potential of IL-27 gene delivery by sonoporation to treat and reduce the growth of prostate cancer *in vivo*. We used three models of immune-competent prostate adenocarcinoma and characterized the tumor-growth reduction, gene-profile expression, and effector cellular profiles. Our results suggest that IL-27 can be effective in reducing tumor growth and can help enhance accumulation of effector cells in prostate tumors *in vivo*. These results are promising, because they are potentially relevant to developing new therapies that can be translated by using the novel and effective sonoporation gene therapy delivery strategy.

Materials and Methods

Cell culture and transfections

Mouse TRAMP-C1 and TRAMP-C2 cells were obtained from ATCC (Manassas, VA) and maintained in Dulbecco's modified Eagle's medium with F12 (DMEM:F12; Mediatech, Manassas, VA) with 10% fetal bovine serum (FBS), 1% penicillin-streptomycin (PS). The RM1 murine prostate cancer cell line was provided by W. Heston (Cleveland Clinic, Cleveland, OH). These cells were originally generated from C57BL/6 mice using the mouse prostate reconstitution model (Thompson *et al.*, 1989) with cells characterized as previously described (Baley *et al.*, 1995). Cells were cultured *in vitro* in DMEM:F12 (Mediatech) with 10% FBS, 1% PS, and regularly passaged by trypsinization [0.05% (vol/vol) trypsin, 0.53 m*M* EDTA]. Conditioned culture medium (CCM) from RM1 cells was obtained as follows: RM1 cells were grown to 70% confluence, washed 2$\times$ in PBS, which was replaced with 2% FBS DMEM:F12 medium, and CCM was collected 24 hr later.

Vectors

Plasmid DNA vectors were prepared using a pORF9 backbone (InvivoGen, San Diego, CA) to generate either empty vector (pORF-0) or humanized renilla luc gene (hRluc) using *Bgl*II and *Xba*I to excise, insert, and place into *Bgl*II and *Nhe*I sites in pORF. The pORF-mIL-27, containing the mouse EBI3 and p28 IL-27 cDNAs in tandem, was obtained from InvivoGen, as was the pORF-luc. Vectors were prepared for all experiments using a Giga Endofree kit (Qiagen, Valencia, CA). Ad-CMV-GFP and Ad-CMV-Luc vectors were from Vector BioLabs (Philadelphia, PA), and amplified using progressively larger Ad293 cell cultures to infect $\sim$70–90% confluent Ad293 cells in 3$\times$150 mm plates. Cytopathic effect (CPE) was collected within 48 hr of infection; cells were lysed by three cycles of freeze-thawing, then centrifuged at 3,000 *g* for 10 min; and the supernatant was purified using the ViraBind Adenovirus (Ad) Purification kit (Cell Biolabs, San Diego, CA) and titered using a Quicktiter Ad immunoassay kit (Cell Biolabs), according to the manufacturer's protocols.

In vivo *studies and molecular bioluminescence imaging (BLI)*

Animal care and procedures were performed in accordance with the Louisiana State University (LSU) institutional review board guidelines. Mouse prostate cancer cells (5×10^3 RM1, 2×10^6 TRAMP-C2 or TRAMP-C1) were delivered subcutaneously in 100 μl of 1$\times$Dulbecco's phosphate-buffered saline (DPBS) to the flanks of 6–8-week-old C57/BL6 male mice (Harlan, Houston, TX). Human prostate cancer cells (10^6 PC3 or DU145) were pelleted by centrifugation at 1,300–1,500 rpm for 5 min, medium was aspirated in a sterile culture hood, and cells were resuspended in 1$\times$DPBS. Cells were delivered in 100 μl of 1$\times$DPBS plus 30 μl of Matrigel (BD Biosciences, San Diego, CA) and implanted subcutaneously in the flanks of 6–8-week-old Balb/c *nu/nu* male mice. The tumor growth was monitored over time using vernier calipers.

For sonoporation, SonoVue MB were obtained from Protech International (Boerne, TX) in lyophilized form and reconstituted in sterile saline to 5 mg/ml. Following testing of several conditions and DNA concentrations, we concurred that the best sonoporation conditions were as follows: with 30% SonoVue, 45–50 μg of plasmid DNA (from a 2 μg/μl stock) in 100 μl/dose in 0.9% sterile PBS, with 2-min irradiation at 1 MHz, 50% duty cycle, 45 V, 2 Hz, and a 6-mm probe using a KTAC 4000 apparatus (Protech International), an intensity of 1 W/cm^2, and an acoustic pressure of 0.12 MPa determined as described (Duvshani-Eshet and Machluf, 2005). Similar conditions for sonoporation have been described for this apparatus (Suzuki *et al.*, 2008, 2010). For therapy studies, four treatments of either sonoporation or Ad, spaced 48 hr

apart, were performed for TRAMP-C2 recipients, where each sonoporation dose was 50 μg of pDNA (total = 200 μg), and the Ad was 2×10^8 particle forming units (pfu; total = 8×10^8 pfu). These doses were based on a recent study by Pislaru and colleagues, whereby $\sim$800 μg of plasmid DNA mixed with Optison MB produced equivalent gene expression levels (as assessed by Luc activity) as $\sim3.3\times10^9$ infectious Ad particles following administration in muscle tissue (Pislaru *et al.*, 2003). This relative equivalency was also supported by a recent study by Passineau and co-workers, where sonoporation of pLuc at a dose equivalent to 45 μg plus Definity MB transfected salivary glands with similar efficiency as an $\sim$10-fold lower Ad amount ($\sim3.5\times10^8$ Ad) (Passineau *et al.*, 2010). We therefore used the findings of these two reports to deliver equivalent doses in our studies. For TRAMP-C1 or RM1 recipients, treatments consisted of sonoporation only. Treatments were administered in the RM1 model on days 2, 4, 6, and 8 post implantation (microscopic tumor treatment), in the TRAMP-C1 model on days 7, 10, 12, and 14 post implantation, and in the TRAMP-C2 model on days 38, 40, 42, and 44 post implantation. For all tumor models, pDNA or Ad was administered intratumorally.

For *in vivo* imaging studies, mice were anesthetized using isoflurane inhalation anesthesia and then received a tail-vein injection of either coelenterazine (5 mg/kg) if the vector used encoded for renilla luciferase or an intraperitoneal injection of luciferin (150 mg/kg) if the vector used encoded for firefly luciferase (luc). Bioluminescence images were collected under isoflurane anesthesia 48 hr post sonoporation using a cooled IVIS50 CCD camera and nose-cone respirator system (Xenogen, Alameda, CA) and analyzed using Igor-PRO Living Image Software 3.2.

Cell growth assay, migration assay, and bone chemotaxic assay

Growth assays were performed in 24-well plates for coculture, colony formation, and Matrigel invasion assays. For assaying cell number increase over time, a cell counting kit (CCK8, Fisher Scientific, Pittsburgh, PA) using 3×10^3 cells in a 96-well plate format was used. Ten microliters of substrate was added, followed by incubation for 2 hr at 37°C, and absorbance was read at 450 nm. For Matrigel invasion assay, 24-well inserts contained 20 μl of 1:6 Matrigel:serum-free medium dilution (BD Biosciences), and 10^5 prostate cancer cells were plated in the top chamber in 0.5 ml of 0.5% FBS Iscove's modified Dulbecco's medium or RPMI 1640. The bottom chamber received 0.5 ml of the same medium with 10% FBS. At 48 hr, inserts were fixed using 10% buffered formalin, and Matrigel was removed with a cotton swab. Membranes were mounted on glass sides using DAPI mounting medium, images were acquired for five to seven independent microscopic fields under a 10× lens using a BC-364 Jenco inverted epifluorescence microscope (Bioexpress, Kaysville, UT), and the total area fraction was covered by cells determined using NIH ImageJ software. An osteoblast coculture assay was performed as described (Zolochevska and Figueiredo, 2011). In brief, 10^5 prostate cancer cell lines were seeded atop an 8-μm transwell insert, and 10^4 MC3T3-E1 clone 4 osteoblasts were seeded at the bottom in osteoblast conditioned medium, comprising a chemotaxis model for bone microenvironment (Wu *et al.*, 2007). Migrating cells were stained with DAPI, and an area fraction (%) for migrating cells was obtained. For each cell line, the fold change over control sample was determined. Bone cell viability was determined using a 0.5% (wt/vol) crystal violet assay and A550 reading for absorbance indicating viable cell staining.

Real-time quantitative RT-PCR (qPCR) analyses

Total RNA from $5–10\times10^5$ cell lines was extracted using a SurePrep kit (Fisher Scientific). Two micrograms total RNA was reverse-transcribed using a TaqMan kit (Applied Biosystems, Foster City, CA). A 1-μl template cDNA was used in a real-time qPCR reaction with 2× Sybr green master mix (Applied Biosystems) and a 10 μM concentration of each forward and reverse primer for experimental or control housekeeping genes. Reactions were run on an ABI7300 cycler (Applied Biosystems), using 40 repeats of 95°C/15 sec, 56°C/30 sec, 72°C/30 sec, and then analyzed using ABI7300 software. All samples were normalized to the internal β-actin control and expressed as change in C_t relative to β-actin. For qPCR array experiments, the PAMM-053A mouse B- and T-cell activation qPCR array was used from SABiosciences (Qiagen) according to the manufacturer's protocols.

Flow cytometry assays

Cells for flow cytometry detection were assayed on a FACScan (BD Biosciences) at the LSU Flow Cytometry Core Facility. Tumor-infiltrating lymphocytes were isolated following four sonoporation treatments *in vivo* 48 hr apart. Either RM1 or TRAMP-C2 tumors were collected 48 hr after the last treatment, and four or five tumors were pooled and minced into small pieces using sterile scalpels in 1×DPBS. Tumor tissue was further dissociated into single cells by incubation in 2.5 mg/ml DNase type II (Fisher Scientific), 1 mg/ml collagenase type IV (Sigma-Aldrich, St. Louis, MO), and 0.5 mg/ml hyaluronidase type V (Sigma-Aldrich) in 1×DPBS for 90 min at 37°C, and strained through a 70-μm mesh. The cell pellet was washed twice in 1× DPBS containing Ca^{2+} and Mg^{2+} (Invitrogen, Carlsbad, CA), with spins at 1,500 rpm for 5 min, strained once more through a 70-μm mesh, resuspended in 1× DPBS containing Ca^{2+} and Mg^{2+}, and counted. Then $2–4\times10^6$ cells were further stained and $\sim2.5–5\times10^5$ cells were collected during the analysis. Cells were stained in cell staining buffer (BioLegend, San Diego, CA), and anti-mouse antibodies (0.25 μg) were used to detect surface marker expression, including Mac1(CD11b)-APC-Cy7, Gr1-FITC, CD8a-FITC, CD3-PE (BioLegend), and CD124(mIL4R)-PE (BD Biosciences). For T regulatory (Treg) cell detection, a kit was obtained with FoxP3-A467, CD25-PE, and CD4-FITC anti-mouse antibodies (BioLegend). Flow cytometry was performed on a Becton Dickinson FACSCalibur using Cell Quest Software (BD Biosciences). The corresponding isotype antibodies were used as controls. Data analysis was performed using FlowJo 9.1 software (Tree Star Inc., Ashland, OR).

Statistical analysis

Assays were performed in triplicate, and values are presented as means ± SEM or 95% confidence interval. Comparisons were performed using an unpaired t test, and $p < 0.05$ was considered to indicate a significant difference.

Results

Sonoporation is efficient in delivering a reporter gene vector to mouse and human prostate tumors

Sonoporation is a relatively novel delivery means for gene therapy. We have established the optimal conditions in the laboratory for delivering reporter gene vectors mixed with SonoVue MB and low-frequency US following intratumoral administration of plasmids. The characterization experiments have included two immune-competent mouse models of prostate cancer (RM1 and TRAMP-C2; Fig. 1), and two immune-deficient human models of prostate cancer (PC3

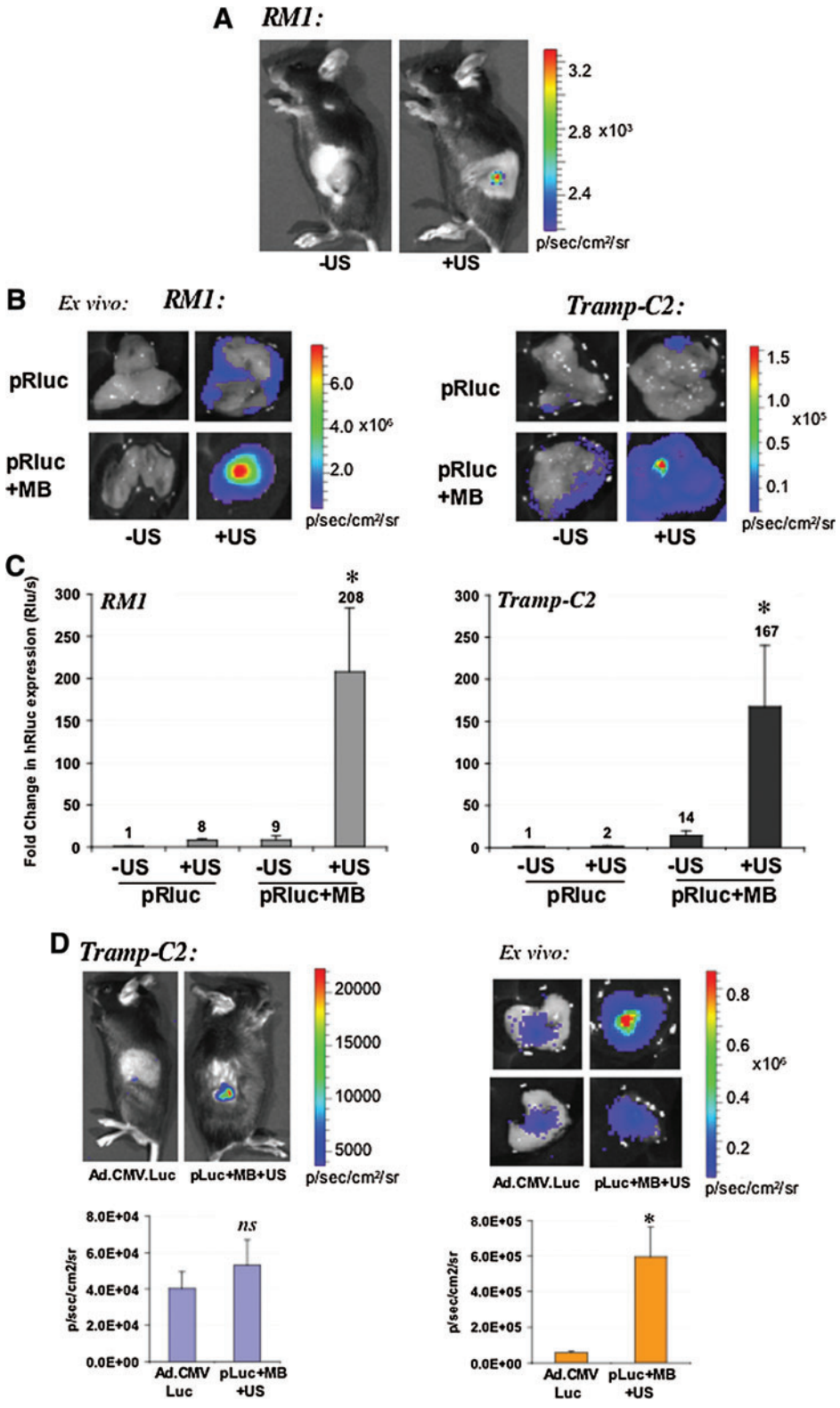

FIG. 1. Characterization of sonoporation gene delivery by BLI in mouse prostate tumor models. **(A)** *In vivo* BLI of mouse RM1 prostate tumors sonoporated with a plasmid encoding renilla luciferase (Rluc). C57/BL6 male mice bearing subcutaneous RM1 prostate tumors received a single dose of pRLuc plus SonoVue and were exposed to no sonoporation or US (–US) or to US (+US) as described in Materials and Methods. Exposure of tumors to sonoporation results in a detectable Rluc signal, whereas the group without sonoporation exposure does not emit a detectable signal *in vivo*. **(B)** *Ex vivo* BLI of mouse RM1 and TRAMP-C2 prostate tumors. Tumors were injected with either naked (pRLuc) or plasmid mixed with SonoVue MB (pRluc+MB) as described in Materials and Methods. Tumors were immediately exposed to US or sonoporation (+US) or left nonirradiated (–US). Shown are the Rluc signals detected. The color bar indicates quantification of the luminescence signal in p/sec/cm^2/sr. **(C)** Fold change in Rluc expression in tumors upon sonoporation. The quantifiable luminescence signals allow calculation of the fold changes in Rluc expression in RM1 and TRAMP-C2 tumor models. Tumors received either pRLuc or pRLuc complexed with SonoVue MB (pRluc+MB), in the absence (–US) or presence of sonoporation or US (+US). *$p < 0.05$. **(D)** Comparison of signals emitted from TRAMP-C2 tumors injected intratumorally with either a single dose of Ad vector (5×10^7 pfu) or 50 μg of plasmid encoding firefly luciferase (pLuc) mixed with SonoVue and sonoporated (pLuc+MB+US). *Left: In vivo* signal detection, color bar, and quantification plot. *Right: Ex vivo* isolated tumor imaging and color bar in p/sec/cm^2/sr, and quantification plot. *$p < 0.005$. Color images available online at www.liebertonline.com/hum

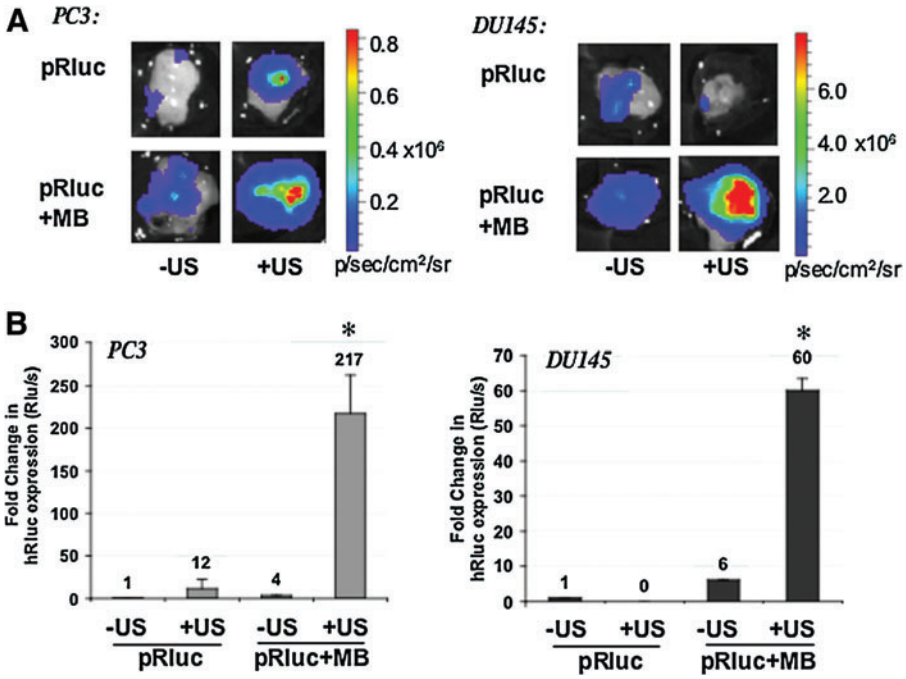

FIG. 2. Sonoporation gene delivery *in vivo* by BLI in human prostate tumor models. **(A)** *Ex vivo* BLI of human PC3 or DU145 prostate tumors sonoporated with a plasmid encoding renilla luciferase (Rluc). Balb/c *nu/nu* male mice bearing subcutaneous PC3 or DU145 prostate tumors received either naked (pRLuc) or plasmid mixed in SonoVue MB (pRluc+MB) as described in Materials and Methods. Tumors were immediately exposed to US or sonoporation (+US) or left nonirradiated (–US). Shown are the Rluc signals detected. The color bar indicates quantification of the luminescence signal in p/sec/cm^2/sr. **(B)** Fold change in Rluc expression in tumors upon sonoporation. The quantifiable luminescence signals allow calculation of the fold changes in Rluc expression in PC3 and DU145 prostate tumor models. Tumors received either pRLuc or pRLuc mixed with SonoVue MB (pRluc+MB) in the absence (–US) or presence of sonoporation or US (+US). *$p<0.05$. Color images available online at www.liebertonline.com/hum

and DU145; Fig. 2). Following intratumoral administration of 50 μg of a plasmid bearing the renilla luciferase reporter gene (pRluc) mixed with 30% SonoVue, tumors were irradiated with low-frequency US as described in Materials and Methods. In the absence of US (–US), a signal cannot be detected by whole-body BLI, whereas in the presence of US (+US), a signal is detectable *in vivo* (Fig. 1A). Upon excision of tumors and *ex vivo* BLI, we observed that US of naked pRLuc (no SonoVue) also could augment its transfection of tumor cells, apparently yielding a detectable signal (Fig. 1B). The addition of SonoVue MB to the DNA resulted in an enhancement in tumor transfection in TRAMP-C2 tumors (Fig. 1B), whereas MB+US resulted in a dramatic enhancement in the transfection of the tumors as shown by an increase in the Rluc signals detected by BLI (Fig. 1B). The magnitude of the changes in Rluc expression are represented in Fig. 1C, where mixing DNA+MB+US resulted in an $\sim$200-fold increase in Rluc expression in RM1, and an $\sim$170-fold increase in TRAMP-C2 tumors. Interestingly, we sought to examine whether an estimated comparable dose of Ad (Pislaru *et al.*, 2003) expressing firefly luciferase (luc) and a plasmid expressing luc could be detectable *in vivo* and *ex vivo*. We observed that the BLI signals were of enhanced magnitude for the DNA+MB+US group (Fig. 1D), suggesting that sonoporation with these optimized conditions may be an attractive alternative to viral methods of gene delivery *in vivo*. Ad-luc *in vivo* total flux signals were on average $\sim 4\times10^4$ p/sec/cm^2/sr, versus pLuc signals of $\sim 5\times10^4$ in TRAMP-C2 tumors; this difference was not significant ($p=0.4$) (Fig. 1D, left panel). The *ex vivo* signals, however, were on average $\sim 6\times10^5$ p/sec/cm^2/sr for pLuc versus $\sim 5.5\times10^4$ p/sec/cm^2/sr ($p<0.005$), suggesting the sonoporation method might be roughly $\sim$10 times more efficient than Ad at the doses used. Importantly, these sonoporation doses or conditions did not yield any histopathology changes in tumors or normal organs of animals (Supplementary Fig. S1; Supplementary Data are available online at www.liebertonline.com/hum).

Although our gene-therapy approach necessitates the use of immune-competent models for examining the effects of interleukin therapy, we also sought to establish whether the sonoporation strategy could efficiently transfect prostate tumors of human origin. For this purpose, we used PC3 and DU145 human prostate cancer cells implanted subcutaneously into *nu/nu* mice. We observed similar effects following sonoporation of pRLuc when DNA+MB+US conditions were used (Fig. 2A). The best tumor transfection occurred with DNA+MB+US, with an $\sim$220-fold increase in Rluc expression for PC3, and an $\sim$60-fold up-regulation in DU145 tumors (Fig. 2B). Interestingly, in DU145 tumors, the exposure of naked DNA to US appeared instead to reduce the transfection efficiency.

IL-27 gene therapy modifies biology of prostate cancer cells

Prior to *in vivo* studies, we examined the potential for IL-27 expression in modifying the malignant characteristics of prostate cancer cells *in vitro*. We observed that transfection of the prostate cancer cell line TRAMP-C2 with a plasmid encoding IL-27 resulted in a reduction in cell viability relative to control empty vector (Fig. 3A) and reductions in the fraction of prostate cancer cells migrating toward a chemotactic stimulus, which reflects the invasiveness potential of a tumor cell line (Fig. 3B). RM1 cells displayed an 80% reduction in the fraction of invasive cells, whereas TRAMP-C2 and TRAMP-C1 cells displayed $\sim$50% reduction in the fraction of invasive cells ($p<0.03$). Another malignant

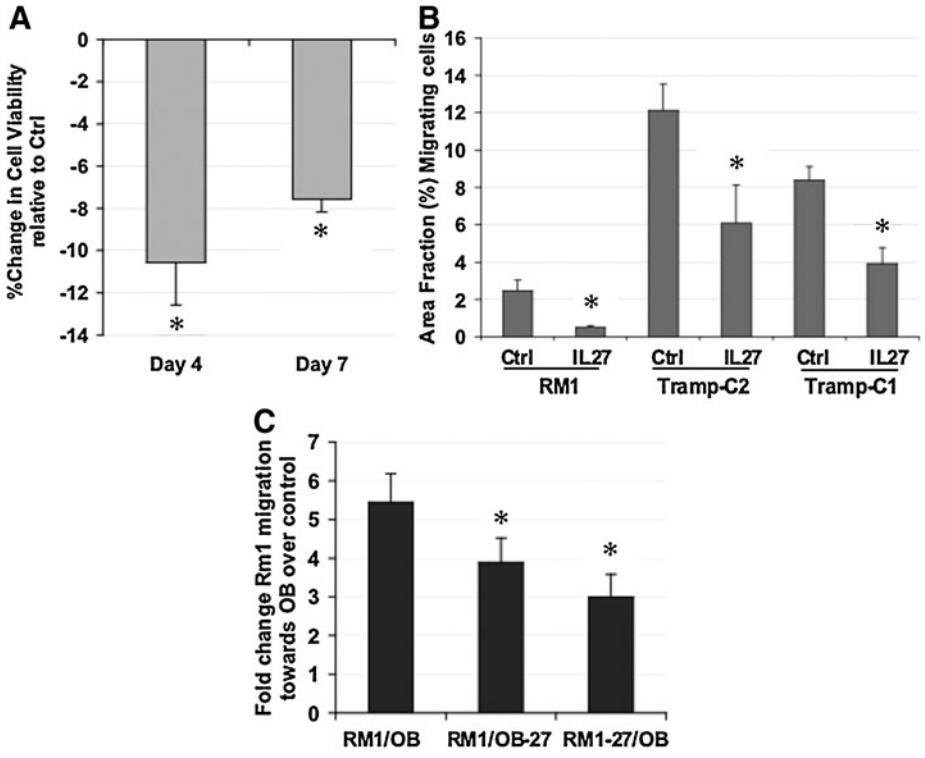

FIG. 3. The effect of novel IL-27 gene-therapy strategy on the biology of prostate cancer cells. **(A)** The effect of IL-27 expression on prostate cancer viability. TRAMP-C2 mouse prostate cancer cells were transfected with either pIL-27 or empty plasmid control. A significant reduction in cell viability can be observed by days 4 and 7 post transfection. *$p < 0.02$. **(B)** IL-27 expression decreases aggressiveness of prostate cancer cells. Transfection of either RM1, TRAMP-C2, or TRAMP-C1 mouse prostate cancer cells with either an IL-27-expressing plasmid or an empty plasmid contol results in a decreased invasive potential for prostate cancer cells in a Matrigel invasion assay. *$p < 0.05$. **(C)** IL-27 expression decreases the ability of prostate cancer cells to migrate toward a bone chemotactic stimulus. Expression of IL-27 in either the osteoblast (OB-27) or the prostate cell (RM1-27) compartment resulted in a significant reduction in migratory ability of RM1 mouse prostate cancer cells. *$p < 0.01$.

characteristic of RM1 cells is their ability to grow aggressively in the bone microenvironment *in vivo* and migrate toward bone cell-derived stimuli *in vitro*. We used our previously described bone chemotactic model for assessing the effect of IL-27 treatment upon cell migration toward osteoblasts in coculture (Zolochevska and Figueiredo, 2011). IL-27 expression in either the RM1 cells or the osteoblasts in coculture prevented migration of RM1 toward osteoblasts (Fig. 3C). In combination, these results suggest that IL-27 expression might be a promising candidate for reducing prostate cancer growth and malignant biological characteristics.

Sonoporation delivery of IL-27 gene therapy reduces prostate tumor growth in vivo

Next we examined the potential of IL-27 gene-therapy delivery by sonoporation strategy in three immune-competent models of prostate cancer in C57/BL6 mice. In the RM1 tumor model, tumor growth occurs very rapidly even from a very small number of implanted cells (5×10^3), signifying the high aggressiveness of this tumor model. Nevertheless, the sonoporation (DNA + MB + US) using pIL-27 (Sono-27) was effective in reducing tumor growth rate by ~50%; these differences were significant between days 14 and 21, the endpoint ($p < 0.04$; Fig. 4A). In the TRAMP-C1 model, a less aggressive but still rapidly growing tumor, Sono-27 appeared to dramatically halt tumor growth up to day 74 post implantation, with some tumors reverting to a faster growth rate at day 78. Overall, the Sono-27 therapy was successful in extending and almost doubling the survival time of treated mice as compared with empty vector control (Sono-ctrl) (Fig. 4B). Finally, we selected the TRAMP-C2 model to examine effectiveness of therapy, as this is a more representative model of the human disease. For instance, TRAMP-C2 tumors retain androgen receptor (AR) expression and display slower growth relative to that of the other two models described,

FIG. 4. Sonoporation-delivered IL-27 gene therapy reduces prostate tumor growth in immune-competent models. **(A)** Intratumoral delivery of IL-27 by sonoporation reduces the growth rate of aggressive RM1 tumors. Four sonoporation treatments, using either control empty plasmid (Sono-ctrl) or pIL-27 (Sono-27), at 50 μg/treatment, were spaced 48 hr apart starting at day 2 post subcutaneous (s.c.) implantation of 5×10^3 RM1 cells in C57/BL6 male mice ($n = 8$/group). Tumor volume (mm^3) was subsequently measured using vernier calipers. *$p < 0.05$. Arrows indicate treatment days. **(B)** Intratumoral delivery of IL-27 by sonoporation reduces growth rate of s.c. TRAMP-C1 tumors and improves survival over time. Four sonoporation treatments (Sono-ctrl or Sono-27, 50 μg/treatment) were spaced 48 hr apart starting at day 7 post s.c. implantation of 4×10^6 TRAMP-C1 cells in C57/BL6 male mice ($n = 8$/group). Tumor volume (mm^3) was subsequently measured using vernier calipers. *$p < 0.02$. Arrows indicate treatment days. **(C)** Intratumoral delivery of IL-27 by sonoporation reduces growth rate of TRAMP-C2 tumors and improves survival over time. Four sonoporation or Ad (control or IL-27) treatments were spaced 48 hr apart starting at day 38 post s.c. implantation of 2×10^6 TRAMP-C2 cells in C57/BL6 male mice. Tumor volume (mm^3) was subsequently measured using vernier calipers ($n = 8$/group). *Left:* Tumor volume plotted as a function of time. *Right:* Relative tumor growth rate calculated as described (Figueiredo *et al.*, 2005). Intratumoral delivery of IL-27 by sonoporation appears to be more effective against s.c. TRAMP-C2 tumors than Ad-IL-27 delivery. *$p < 0.05$. Arrows indicate treatment days.

RM1 and TRAMP-C1. In the TRAMP-C2 model, we expanded our analysis to compare the efficacy of Sono-27 with the Ad-27 therapy. Interestingly, all the control groups (no DNA, Sono-luc, or Ad-luc) displayed similar growth curves, whereas Ad-27-treated tumors grew as a trend faster than its control, Ad-luc (Fig. 4C), but this difference was only significant for day 57 ($p < 0.04$). In contrast, Sono-27 therapy was effective in reducing the growth of TRAMP-C2 tumors compared with the Sono-luc control; this difference was significant at time points between day 47 and day 62, the endpoint for control

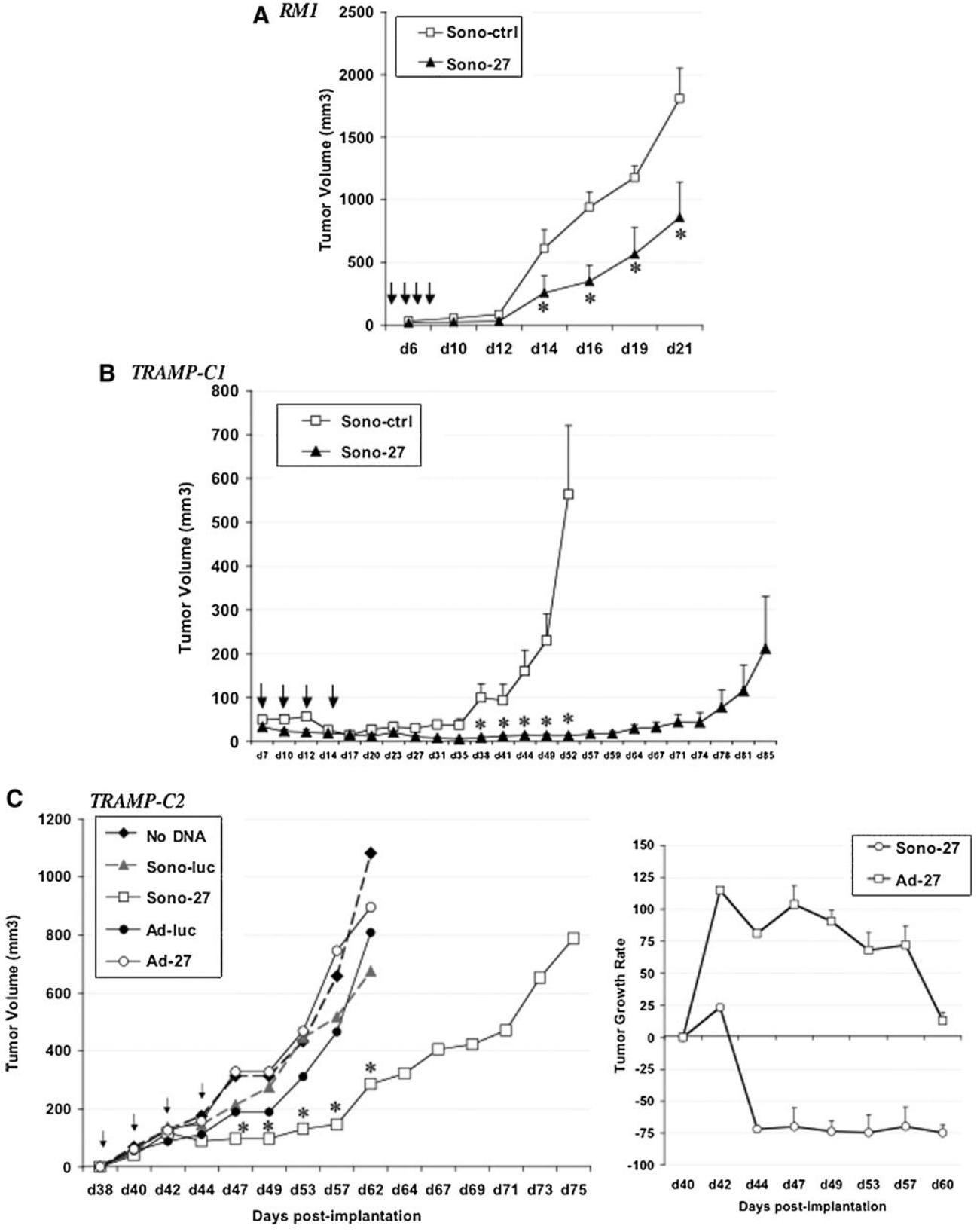

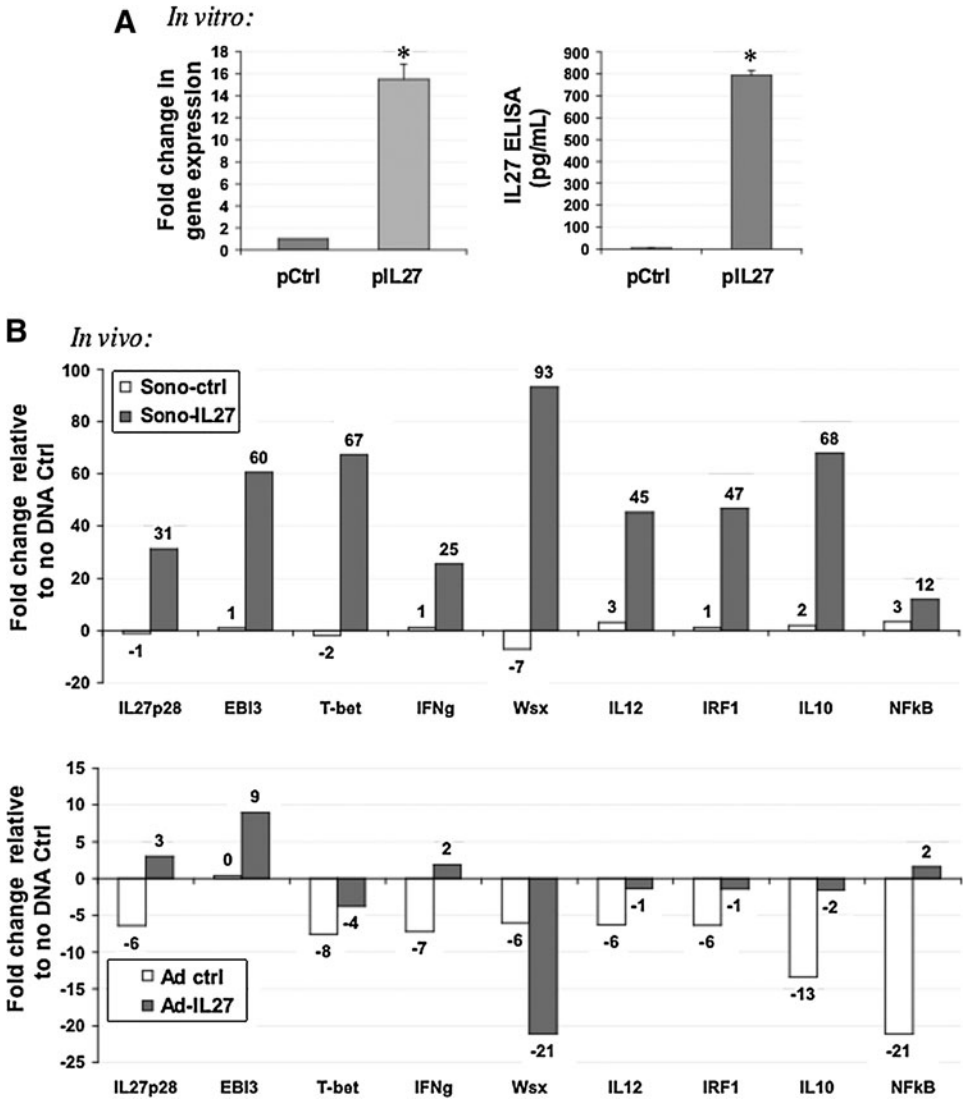

FIG. 5. Differential modulation of IL-27 pathway genes in sonoporation- versus Ad-treated prostate tumors. **(A)** TRAMP-C2 cells express high levels of IL-27 p28 *in vitro* at 48 hr post transfection as detected by real-time PCR using cell lysates and ELISA using conditioned cell media. These results suggest the vector highly up-regulates IL-27 gene expression in prostate tumor cells. $^*p < 0.0002$. **(B)** TRAMP-C2 tumors treated *in vivo* with four treatments of sonoporated control (Sono-ctrl) or IL-27 plasmid (Sono-27) mixed with SonoVue as described in Materials and Methods. Treated tumors up-regulated a host of IL-27 pathway–related genes, including IL-27. In contrast, tumors treated with Ad-IL-27 showed a down-regulation of most related genes, except for modest up-regulation of IL-27, EBI3, and IFNγ. Both plots reflect the fold change in gene expression in each group relative to a "no DNA" tumor control.

animals. Sono-27 also enhanced survival of treated mice, with a 1.2-fold increase in survival time (Fig. 4C, left panel). Tumor growth rate calculations of the Sono-27- or Ad-27-treated tumors relative to their respective controls showed that only the Sono-27 therapy was effective in reducing the tumor growth rate, comprising ~75% reduction (Fig. 4C, right panel). Ad-27 was ineffective in reducing tumor growth and, in fact, as a trend enhanced the tumor growth rate as compared with the Ad-luc control, although this difference was only significant at day 57.

Sonoporation delivery of IL-27 induces a profile of expression of IL-27 pathway–related genes

We examined the profile of gene expression relating to the IL-27 pathway and observed that IL-27 is expressed upon transfection with plasmid DNA in TRAMP-C2 cells *in vitro*, as assessed by real-time qPCR and ELISA (Fig. 5A). Levels of gene expression were increased ~16-fold, and ELISA detected IL-27 in culture conditioned media at ~270-fold higher levels compared with control ($p < 0.0002$). *In vivo*, we observed a dramatic up-regulation in IL-27, EBI3, and Wsx genes, and also the downstream effectors of IL-27 function, T-bet, IFNγ, and IRF1. Other related genes up-regulated by Sono-27 were IL-12, IL-10, and nuclear factor-κB (NFκB). Although the Ad-27 therapy also could up-regulate IL-27, EBI3, IFNγ, and NFκB, the up-regulation observed was more modest than that induced by Sono-27 (Fig. 5B).

Sonoporation delivery of IL-27 in vivo *induces a gene-expression profile suggestive of immune effector cell activation in prostate tumors*

We compared the profile of gene expression activated by either Sono-27 or Ad-27 therapies *in vivo* in TRAMP-C2 tumors using a B- and T-cell activation qPCR array. We observed interesting changes that could be consistent with T-cell activation, differentiation, and proliferation in tumors (Table 1). For *T-cell activation*, common alterations induced by both Sono-27 and Ad-27 therapies were up-regulation of Irf4, Cd8a, Cd8b1, and Sit1. Opposing changes were up-regulation of Cd1d1, Cd3d, and Vav1 by Sono-27, whereas in Ad-27-treated tumors these genes were down-regulated. Tnfsf14 was down-regulated in Sono-27 and up-regulated in Ad-27. Other gene alterations observed for Sono-27 only

Table 1. IL-27 Therapies Modulate a Gene-Expression Profile Suggestive of Immune Cell Effector Activation or Proliferation *In Vivo*

	Genes up-regulated (fold change)		*Genes down-regulated (fold change)*	
Function	*Sono-27*	*Ad-27*	*Sono-27*	*Ad-27*
T-cell activation	**Sit1** (15.8) **Irf4** (4.9) **Cd8a** (2.0) **Cd8b1** (3.3) Cblb (1.8) Cd1d1 (8.1) Cd3d (1.6) Vav1 (1.7) Dock2 (7.1) Cd2 (4.1)	**Sit1** (2.3) **Irf4** (6.1) **Cd8a** (12) **Cd8b1** (13) Tnfsf14 (3.8) Icos1 (3.9)	Tnfsf14 (–4.8)	Cd1d1 (–2.1) Cd3d (–3.2) Vav1 (–7.2) Prlr (–32) Was (–2.7)
T-cell proliferation	**IL-10** (10.2) Cd3e (15.4) Dock2 (7.1) IL-12b (1.5) Tnfr sf13c (3.9)	**IL-10** (6.8) Pdcd1lg2 (12) Tnfsf13b (11) Tnfsf14 (3.8) Cxcl12 (3.9)		Cxcr4 (–15) Dock2 (–2.0) IL15 (–5.2) Ptprc (–11) Sftpd (–3.0)
T-cell differentiation	**IL-27** (7.3) **Irf4** (4.9) **Jag2** (5.8) Ap3b1 (6.0) Bad (9.2) Cd1d1 (8.1) Cd2 (4.1) Cd3d (1.6) Dock2 (7.1) Gadd45g (3.0) IL-12b (1.5)	**IL-27** (1.5) **Irf4** (6.1) **Jag2** (15) Nos2 (4.0)	Pawr (–4.2)	Gadd45g (–9.0) Ptprc (–11) Cd1d1 (–2.1) Cd3d (–3.2) IL-15 (–5.2)
Th1/Th2 differentiation	*Cd28* ***(9.8)*** *IFN* γ ***(5.0)*** IL-12b (1.5)	**Cd28** (22.4) **IFN** γ (7.2) Cd40lg (20)		

Text in "bold" indicates gene-expression changes common to both IL-27 therapies. For all changes presented, $p < 0.05$.

included up-regulation in Cd2, Cblb, and Dock2. For Ad-27, Icos1 was up-regulated and Prlr and Was were down-regulated. For *T-cell proliferation*, the only common alteration to both Sono-27 and Ad-27 therapies was IL-10 up-regulation. Opposing changes were up-regulation of Dock2 in Sono-27, whereas this gene was down-regulated in Ad-27. Other gene expression alterations for Sono-27 were up-regulation of Cd3e, IL-12b, and Tnfrsf13c. For Ad-27, Pdcd1lg2, Tnfsf13b and 14, and Cxcl12 were up-regulated and Cxcr4, IL-15, Ptprc, and Sftpd were down-regulated. For *T cell differentiation*, common alterations were IL-27, Irf4, and Jag2 up-regulation, and opposing changes were up-regulation of Cd1d1, Cd3d, and Gadd45g in Sono-27 with down-regulation in Ad-27. Other Sono-27 gene alterations were up-regulation of Ap3b1, Bad, Cd2, Dock2, and IL-12b, and down-regulation of Pawr. For Ad-27, Nos2 was up-regulated, whereas Ptprc and IL-15 were down-regulated. For *Th1/2 differentiation*, common changes observed between Sono-27 and Ad-27 were up-regulation of Cd28 and IFNγ. Sono-27 up-regulated IL-12b, whereas Ad-27 up-regulated Cd40lg. In combination, these results may point to clues as to key mechanistic differences in therapeutic effectiveness between Sono-27 and Ad-27, suggesting differences in gene expression related to T-cell activation, proliferation, and differentiation.

Sonoporation delivery of IL-27 modifies effector cell accumulation in prostate tumors

In RM1 tumors treated with Sono-27, we observed a dramatic increase in $CD3^+CD8^+$ cells, suggesting an increase in tumor-infiltrating lymphocytes as compared with control (Fig. 6A). Sono-27 enhanced the percentage of $CD3^+CD8^+$ cells by $\sim$120% over Sono-ctrl. Also observed were decreases in $Gr1^+CD11b^+CD124^+$ and $Gr1^+Cd11b^+$ populations, suggesting a decrease in myeloid derived suppressor cells (MDSC) ($p < 0.03$) (Fig. 6B). Cells of a potential Treg population staining for $CD4^+CD25^+$ $FoxP3^+$ were reduced by $\sim$50% in RM1 tumors ($p < 0.001$) (Fig. 6C).

In TRAMP-C2 tumors, we compared the Sono-27, Ad-27, and control therapies and their ability to recruit effector cells to the tumor microenvironment. We observed a dramatic increase in $CD3^+CD8^+$ cells in Sono-27-treated tumors (Fig. 7A). Ad control treatment also increased numbers of this cell population, although at three times lower levels than Sono-27 (Supplementary Fig. S2). The Ad-27 therapy showed a reduced number of this cell population (Fig. 7A). This discrepancy in the ability of different IL-27 therapies to recruit $CD3^+CD8^+$ cells to tumors might be a mechanism in the different therapeutic efficacies observed (*i.e.*, Sono-27 is

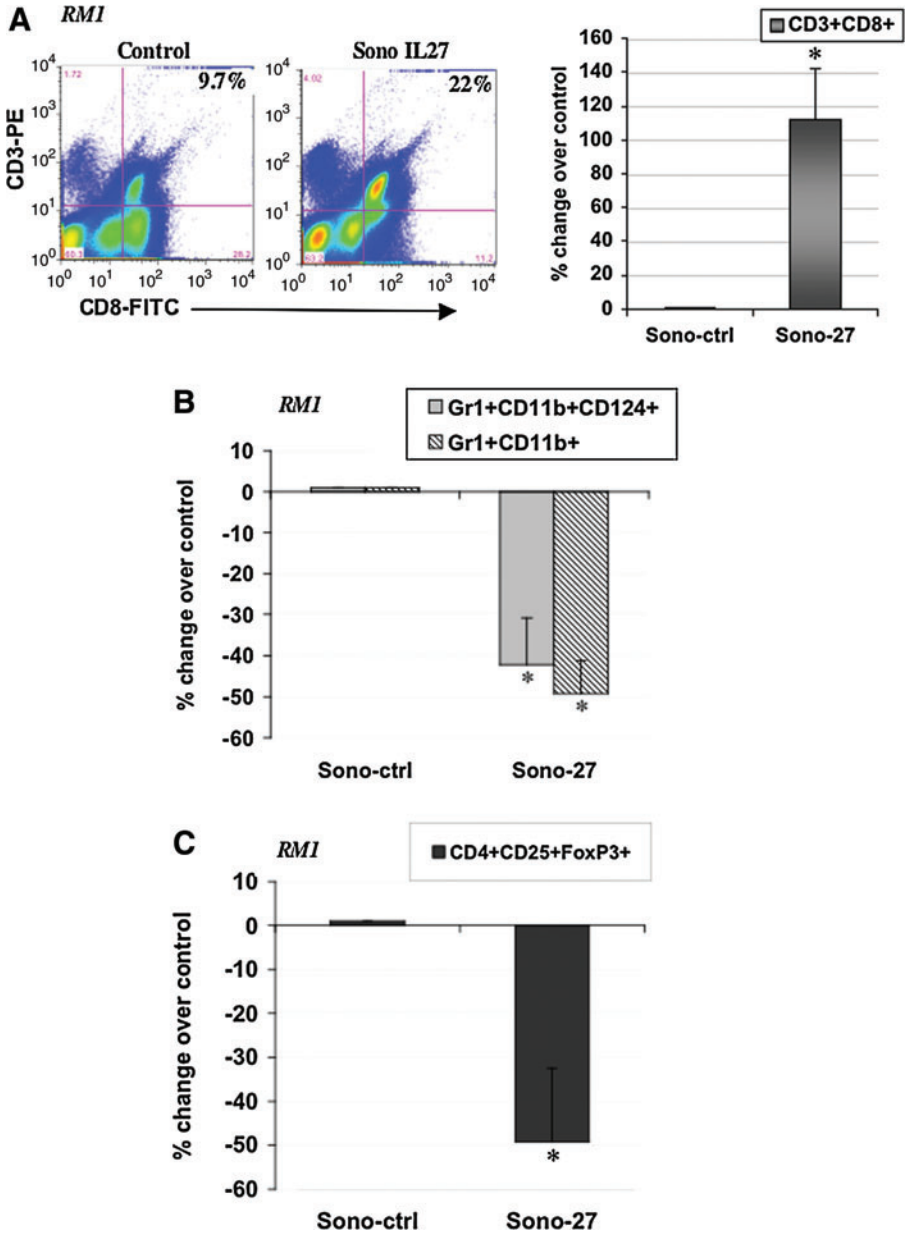

FIG. 6. Modulation of immune effector cell accumulation in RM1 prostate tumors by IL-27 sonoporation (Sono-27) *in vivo*. **(A)** Increased accumulation of $CD3^+CD8^+$ T cells was observed in RM1 tumors treated with four sonoporation treatments as described in Materials and Methods. *Left:* Flow cytometry data. *Right:* The percent change observed over control (tumors sonoporated with control empty plasmid). $^*p<0.009$. **(B)** Decreased accumulation of $Gr1^+CD11b^+CD124^+$ cells ($p<0.03$) was observed in Sono-27-treated RM1 tumors, and proportions of $Gr1^+CD11b^+$ cells ($p<0.002$) were also reduced. **(C)** Decreased accumulation of $CD4^+CD25^+FoxP3^+$ cells ($p<0.001$) was observed in Sono-27-treated RM1 tumors. Color images available online at www.liebertonline.com/hum

effective in reducing tumor growth, whereas Ad-27 is refractory). MDSC populations were detected at reduced levels in Sono-27- and Ad-27-treated tumors (Fig. 7B), although with some variations. Sono-27 as a trend reduced levels of $Gr1^+CD11b^+$ ($p=0.13$) and significantly reduced $Gr1^+CD11b^+CD124^+$ ($p<0.006$), and Ad-27 reduced both $Gr1^+CD11b^+$ and $Gr1^+CD11b^+CD124^+$ significantly ($p<0.03$) in TRAMP-C2 tumors (Fig. 7B). Ad control therapy dramatically enhanced the MDSC populations in tumors (Supplementary Fig. S2). Both Sono-27 and Ad-27 also had reduced levels of the potential Treg cell population expressing $CD4^+CD25^+FoxP3^+$ ($p<0.03$ for both therapies) (Fig. 7C). Since Ad control had some effects on enhancing MDSC and Treg cells, the viral vector itself might have an immune-suppressive effect in the tumor microenvironment. Overall, we suggest that the Sono-27 therapy appears to induce changes in the tumor microenvironment in a distinct manner from Ad-27 and is especially more effective potentially due to the recruitment of $CD3^+CD8^+$ cells into prostate tumors.

Discussion

Virtually all of the existing US-based clinical cancer treatments are based on hyperthermic ablation. The relatively novel concept of using subtler, low-frequency US-triggered phenomena such as sonoporation has a tremendous potential for safely delivering novel cancer treatment modalities. With sonoporation, the low US frequency does not directly stimulate a significant therapeutic effect on the target, but rather is used to deliver a specific treatment. Sonoporation advantages include the ability to deliver not only gene therapy but also chemotherapy, and MB agents can also be engineered to achieve molecular targeting (Lentacker *et al.*, 2009; Phillips *et al.*, 2010; Escoffre *et al.*, 2011). The degree of precision

offered by such a capability might permit noninvasive spatiotemporal therapeutic approaches to address challenges presented by variable tumor architecture or in cases where surgical treatment is contraindicated, such as in bone metastases of cancer. Therefore, the promise of sonoporation as a delivery strategy for gene therapy and other therapeutic means is deemed to be very high in the near future.

In terms of applying sonoporation as a means to deliver plasmid DNA *in vivo*, a number of reports have developed the proof-of-principle data *in vivo* whereby reporter gene expression can be augmented when plasmid DNA is mixed with MB and tumor or muscle tissues are exposed to low-frequency US stimuli. For example, sonoporation has been used to deliver reporter genes encoding B-galactosidase (Hauff *et al.*, 2005), enhanced green fluorescent protein (Tsai *et al.*, 2009), and luciferase (Aoi *et al.*, 2008; Li *et al.*, 2009). These sonoporation approaches are also being applied to cancer therapy. In one study, a herpes simplex thymidine kinase (HSVtk) suicide gene therapy strategy demonstrated the effectiveness of US in facilitating transfer and expression of HSVTK, with dramatic reductions in tumor size upon gancyclovir administration (Aoi *et al.*, 2008). Other studies have used sonoporation-based strategies to deliver immunomodulatory cytokine gene therapy encoding IFNγ (Sakakima *et al.*, 2005) or IL-12 (Suzuki *et al.*, 2010), with significant tumor size reductions in mouse models of hepatocellular and ovarian carcinoma, respectively. Liver metastasis regression was accomplished by combined therapy of an NFκB oligodeoxynucleotide decoy delivered by sonoporation and transportal injection of paclitaxel (Azuma *et al.*, 2008). Based on these studies and our present report, we suggest that sonoporation gene transfer might offer significant potential as a cancer therapy, and the effects of cytokines or other therapies might be augmented if used in combination with chemotherapy-based approaches.

In the present report, we describe for the first time, to our knowledge, the use of sonoporation for delivering either reporter or cytokine genes in prostate cancer models. Also, we present the novel approach of using the IL-27 cytokine gene therapy for treating prostate cancer. We characterized the sonoporation strategy in several models of mouse or human prostate tumor xenografts, observing that this strategy can be efficient in delivering reporter genes mixed with SonoVue MB with a 60- to 200-fold increase in gene expression, as compared with either MB alone or naked DNA in the presence or absence of US. Interestingly, when we compared a viral system with the sonoporation system, we observed at least a similar range of bioluminescent signal detection *in vivo* and in *ex vivo* tumors, with the sonoporation strategy perhaps being more effective in delivering the Luc reporter gene. We used equivalent amounts of virus and plasmid DNA based on previously characterized *in vivo* reporter gene activity, where reporter gene expression was compared between an Ad-luc and pLuc+Optison MB

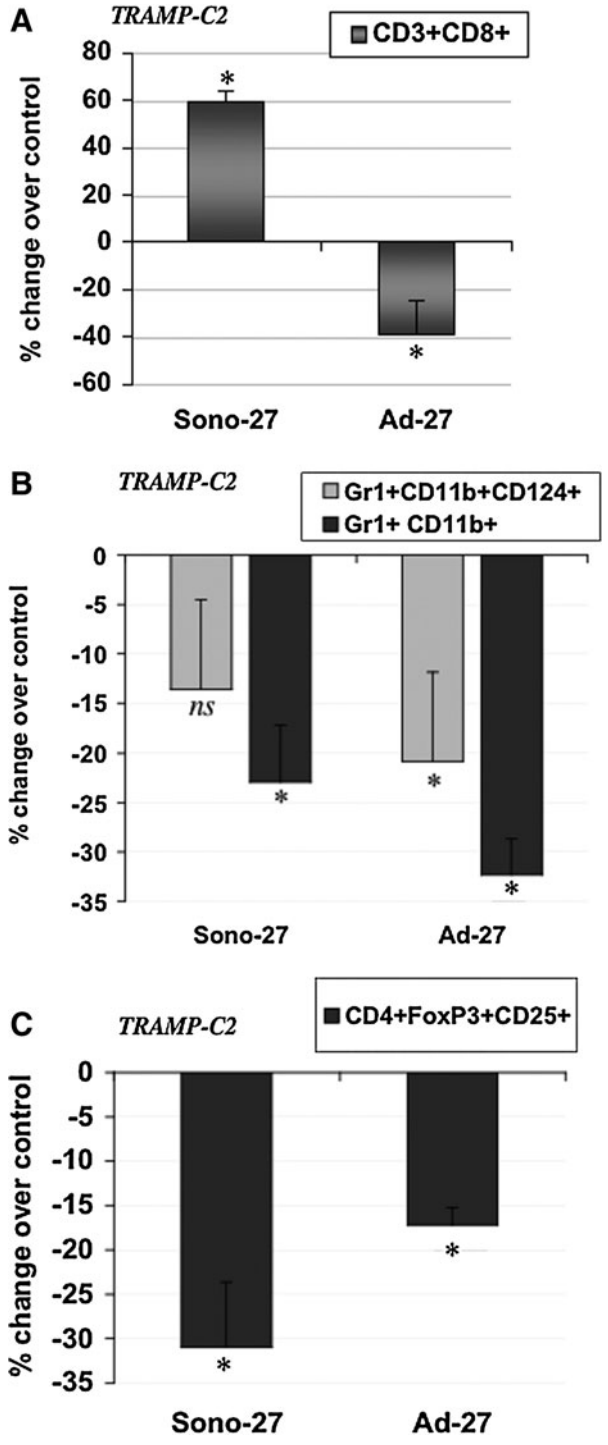

FIG. 7. Modulation of immune effector cell accumulation in TRAMP-C2 prostate tumors by IL-27 sonoporation or Ad therapy *in vivo*. **(A)** Increased accumulation of $CD3^+CD8^+$ T cells was observed in TRAMP-C2 tumors treated with sonoporation IL-27 therapy (Sono-27; $p<0.03$) as described in Materials and Methods. In sharp contrast, in Ad-27-treated tumors, a reduction in $CD3^+CD8^+$ was observed instead ($p<0.04$). Presented is the percent change observed for each treatment group as compared with the respective control groups. **(B)** Reduced accumulation of MDSC populations was observed for both Sono-27- and Ad-27-treated TRAMP-C2 tumors. Sono-27 reduced accumulation of $Gr1^+CD11b^+CD124^+$ cells as a trend ($p=0.13$) and reduced $Gr1^+CD11b^+$ cells ($p<0.03$), whereas Ad-27 reduced $Gr1^+CD11b^+CD124^+$ ($p<0.006$) and $Gr1^+CD11b^+$ populations ($p<0.03$). **(C)** Reduced accumulation of potential Treg population. Both Sono-27 and Ad-27 reduced $CD4^+CD25^+FoxP3^+$ populations ($p<0.03$) in treated TRAMP-C2 tumors.

delivered to muscle tissue (Pislaru *et al.*, 2003). Optison and SonoVue MB have been shown to mediate transfection of pLuc in muscle and tumor with similar efficiencies following sonoporation (Tsai *et al.*, 2009). Our results suggest that although the exact equivalency in dosage between Ad and sonoporated plasmids is difficult to achieve, at the doses used (Pislaru *et al.*, 2003; Passineau *et al.*, 2010), our imaging data suggested that the sonoporation method can be about four times (*in vivo*) to ~10 times (*ex vivo*) more efficient than Ad. Additionally, we observed that Ad-27 gave threefold induction of IL-27 in tumors, whereas Sono-27 gave 30-fold IL-27 induction, further suggesting that perhaps exact dose equivalency was not reached in this study. Future studies will examine a wider range of doses between Ad and sonoporated plasmids to better characterize the equivalency between these two delivery methods.

Following characterization of sonoporation with reporter genes, we pursued the application of sonoporation *in vivo* to deliver constructs expressing the IL-27 gene. *In vitro*, we had confirmed the literature reports by which IL-27 presents several promising antitumor activities in other cancer cell types, such as breast and colon carcinomas (Zhu *et al.*, 2010). We observed that IL-27 could effectively reduce prostate cancer cell viability, reduce prostate cancer cell invasiveness, and reduce their ability to migrate toward bone chemotactic stimuli. *In vivo*, IL-27 delivery by sonoporation markedly reduced the growth rate in three relatively aggressive immune-competent models of prostate adenocarcinoma. The most aggressive model used was the RM1 (Ras-myc) model, a rapidly growing model in which even a very small number of implanted cells (5×10^3) develop into large tumors within 3 weeks. Even in the RM1 model, we could observe the promise of the IL-27 therapy, where it reduced the tumor growth rate by 50%. In the TRAMP-C1 model, we observed a dramatic halting of tumor growth up to day 74 post implantation, although some tumor regrowth was observed between days 78 and 85 post implantation. We further selected TRAMP-C2 as a more representative model of the human disease, because it retains AR expression and is of a slower relative growth than the other two models. In the TRAMP-C2 model, we tested the efficacy of IL-27 delivered either by sonoporation (Sono-27) or by Ad (Ad-27) as compared with plasmid or Ad controls. Surprisingly, Ad-27 adversely affected tumor growth at least at one time point, and was ineffective, whereas Sono-27 was effective in reducing TRAMP-C2 tumor growth rate by ~75%.

Based on the known effects of IL-27 in facilitating recruitment of immune effector cells in several tumor models, we sought to characterize some potential mechanisms of antitumor action in prostate cancer models. First, using the TRAMP-C2 model, we investigated whether genes related to the IL-27 pathway were overexpressed in tumors. Sono-27 up-regulated IL-27, EBI3, Wsx, and downstream effectors of IL-27 function such as T-bet, IFNγ, IRF1, and also IL-12, IL-10, and NFκB. And although Ad-27 up-regulated IL-27, EBI3, IFNγ, and NFκB, the effect was much more modest than that observed with Sono-27. This would suggest that the differences between Ad-27 and Sono-27 therapies might at least involve different patterns of IL-27-related gene expression. Second, we sought to determine whether IL-27 therapy induced any detectable gene-expression changes related to immune cell infiltration or activation in tumors. For this purpose, we used a qPCR array analysis directed at detecting changes in gene expression related to immune cell activation, proliferation, or differentiation, using TRAMP-C2 tumor samples treated with either Sono-27, Ad-27, or appropriate controls. From the panel of genes represented in the array, we observed that IL-27 therapy induced gene-expression changes clustering mostly with T-cell activation, differentiation, and proliferation genes. In some cases, the Ad-27 and Sono-27 therapies had overlapping gene up-regulation, such as Cd8a, Cd8b1, Irf4, suggesting both therapies could induce IL-27 expression and also some level of T-cell activation–related gene expression in tumors. IL-27 was also up-regulated by both therapies, although levels achieved with Sono-27 were approximately seven times higher than those with Ad-27. Other common gene-expression changes were up-regulation of Cd28, Jag2, IFNγ, and IL-10 genes associated with T-cell proliferation and Th1/2 differentiation. Aspects of gene expression that might be responsible for the different therapy efficacies could be related to the opposing gene-expression changes observed. For example, Cd1d1, Vav1, Gadd45g, Cd3d, and Dock2 were up-regulated by Sono-27, but were down-regulated by Ad-27. Sono-27 also up-regulated Cd3d and Cd3e genes, suggesting induction of T-cell activation or proliferation within tumors.

Based on the gene expression data, we pursued other experiments to potentially confirm the presence of certain cell populations within tumors that may underlie the effectiveness of IL-27 therapy *in vivo* following Sono-IL-27. Using surface marker-specific antibodies, we observed an increase in the $CD3^+CD8^+$ T-cell population isolated from both RM1 and TRAMP-C2 tumors. This result was in concordance with the literature on the effects of IL-27 on enhancing T-cell infiltration in tumors, whereby IL-27 can augment CD8 infiltration if administered following IL-12 treatment in CT26 colon tumors (Zhu *et al.*). We also examined the effect of IL-27 therapy in potentially reducing infiltration of immune-suppressive cell populations in tumors. Defective immune function is an important cause of tumor development, and accumulation of MDSC, which inhibit T-cell activity, contributes to the immune suppression characteristic of most tumors. In RM1, the proportion of two potential MDSC populations was reduced ($Gr1^+CD11b^+CD124^+$ and $Gr1^+CD11b^+$). However, the $CD124^+CD11b^+$ population was increased. CD124, the IL-4 receptor α-chain, has been reported to be expressed on MDSC from tumor-bearing mice (Gallina *et al.*, 2006). CD124-expressing cells are typically inflammatory-type monocytes elicited by growing tumors and activated by IFNγ released from T lymphocytes. $CD11b^+CD124^+$ cells can produce IL-13 and IFNγ and integrate the downstream signals of these cytokines to trigger suppression of $CD8^+$ T cells. The expression of CD124 has been shown to be highest on $CD11b^+$ $Gr1^{dull}$ MDSC derived from mice with established tumors (Gallina *et al.*, 2006), suggesting that MDSC might change their phenotype during tumor development and become more suppressive. This result suggests that a potentially more suppressive population of MDSC might form in the RM1 tumors, which could help explain why the Sono-27 therapy has a relatively weaker effect in reducing the growth rate in RM1 tumors (50%) as compared with the TRAMP models (80%) (Fig. 4).

IL-27 may use different antitumor pathways, depending on the microenvironment that particular tumors create.

Therefore, we also examined the proportion of Treg cells in tumors following therapy. Treg cells are part of the T-cell repertoire that keeps the immune system in check by inhibiting proliferation and function of T cells. Treg cells express Foxp3, a transcription factor that controls their development and function. Besides Foxp3 Treg cells, there are Tr1 and Th3, characterized by secretion of immune-suppressive IL-10 and transforming growth factor-β. In a clinical setting, a high number of Treg cells is a poor prognosis indicator, as tumors enhance Treg number as a mechanism to evade tumor recognition (Ghiringhelli *et al.*, 2005). Treg cells suppress CD8 T-cell proliferation and inhibit NK function. As IL-27 has been shown to suppress the number of inducible Treg cells *in vitro* (Neufert *et al.*, 2007; Huber *et al.*, 2008), we examined the proportion of putative Treg cells in tumors treated with IL-27. The mechanistic cues on how IL-27 in some instances promotes a proinflammatory environment by reducing Treg numbers (Neufert *et al.*, 2007; Huber *et al.*, 2008), whereas in others it promotes an anti-inflammatory environment by neutralizing IL-6-induced T-cell proliferation and inducing Tr1 cells, still needs to be clarified (Bettelli *et al.*, 2006; Awasthi *et al.*, 2007; Fitzgerald *et al.*, 2007). In RM1 tumors, the proportion of $CD4^+CD25^+$ $FoxP3^+$ cells was reduced by Sono-27 therapy.

We further selected TRAMP-C2 to examine the effectiveness of Sono-27 versus Ad-27 therapies; this model was chosen as it is more representative of the human disease growth rate and progression. For instance, TRAMP-C2 tumors retain AR expression and display slower growth relative to that of the other two models described, RM1 and TRAMP-C1. Therefore, in TRAMP-C2, the proportion of $CD3^+CD8^+$ cells increased with Sono-27 by $\sim$60% over control, as similarly observed for the RM1 tumor model. Ad-27 apparently was ineffective in inducing accumulation of this cell population in treated tumors ($-$40%) (Fig. 7A). This result suggests that the ability of Sono-27 to induce accumulation of a $CD3^+CD8^+$ T-cell population in treated tumors might be responsible for its higher antitumor efficacy. For the putative MDSC or Treg cell populations, both Sono-27 and Ad-27 reduced cell accumulation in treated tumors. Some differences in the cell populations reduced were apparent between Sono-27 (reduced $Gr1^+CD11b^+$) and Ad-27 (reduced $Gr1^+CD11b^+$ $CD124^+$ and $Gr1^+CD11b^+$).

Despite a promising effect in the present study, IL-27 was not completely effective in eradicating prostate tumors *in vivo*. We propose the effectiveness of IL-27 might depend on the proliferation rate and initial tumor size, whereby microscopic tumor treatment or treatment of small metastases might fare better than treatment of a relatively large tumor mass. Nevertheless, using one single cytokine for immunotherapy may not be effective in eradicating very aggressive tumors, and effectiveness certainly could be boosted by combination with other molecules capable of enhancing the $CD3^+CD8^+$ or other effector cell responses. For example, in breast and colon carcinoma models, IL-27 greatly boosts the antitumor activity of IL-12 if administered sequentially, but is otherwise ineffective against aggressive 4T1 breast cancer *in vivo* (Zhu *et al.*, 2010). In that study, IL-12 plasmid DNA was delivered through intramuscular electroporation followed by IL-27 plasmid administration 10 days later. This treatment schedule fully eradicated (100%) IL-12-sensitive CT26 tumors and also partially eradicated (33%) IL-12-insensitive 4T1 tumors in treated mice. Interestingly, the opposite therapy sequence or monotherapies were less effective. The IL-12 + IL-27 sequential gene therapy was found to induce higher levels of cytotoxic T-lymphocyte activity, increased T-cell infiltration into tumors, and by yielding a large number of tumor-specific $IFN\gamma^+$ CD8 T cells compared with IL-12 alone. Notably, depletion of either T or NK cells during the IL-27 treatment phase reversed tumor eradication, suggesting a potential NK-cell requirement for this sequential gene therapy–mediated tumor eradication. Therefore, future studies might include examination of the effects of IL-12 + IL-27 sequential therapy combination on prostate-tumor therapy by sonoporation to augment the cellular responses observed and potentially eradicate treated tumors *in vivo*.

Acknowledgments

We thank Dr. Marilyn Dietrich for assistance with flow cytometry data collection and analyses, and Dr. Denada Dibra for sharing protocols for the isolation of infiltrating lymphocytes from tumor tissues.

Author Disclosure Statement

The authors have no conflicts of interest to declare.

References

Aoi, A., Watanabe, Y., Mori, S., *et al*. (2008). Herpes simplex virus thymidine kinase-mediated suicide gene therapy using nano/microbubbles and ultrasound. Ultrasound Med. Biol. 34, 425–434.

Awasthi, A., Carrier, Y., Peron, J.P., *et al.* (2007). A dominant function for interleukin 27 in generating interleukin 10-producing anti-inflammatory T cells. Nat. Immunol. 8, 1380–1389.

Azuma, H., Tomita, N., Sakamoto, T., *et al.* (2008). Marked regression of liver metastasis by combined therapy of ultrasound-mediated NF κB-decoy transfer and transportal injection of paclitaxel, in mouse. Int. J. Cancer 122, 1645–1656.

Baley, P.A., Yoshida, K., Qian, W., *et al.* (1995). Progression to androgen insensitivity in a novel in vitro mouse model for prostate cancer. J. Steroid Biochem. Mol. Biol. 52, 403–413.

Bettelli, E., Carrier, Y., Gao, W., *et al.* (2006). Reciprocal developmental pathways for the generation of pathogenic effector TH17 and regulatory T cells. Nature 441, 235–238.

Deshpande, N., Needles, A., and Willmann, J.K. (2010). Molecular ultrasound imaging: current status and future directions. Clin. Radiol. 65, 567–581.

Duvshani-Eshet, M., and Machluf, M. (2005). Therapeutic ultrasound optimization for gene delivery: a key factor achieving nuclear DNA localization. J. Control. Release 108, 513–528.

Engel, M.A., and Neurath, M.F. (2010). Anticancer properties of the IL-12 family—focus on colorectal cancer. Curr. Med. Chem. 17, 3303–3308.

Escoffre, J.M., Piron, J., Novell, A., and Bouakaz, A. (2011). Doxorubicin delivery into tumor cells with ultrasound and microbubbles. Mol. Pharm. 8, 799–806.

Feril, L.B., Jr., Ogawa, R., Tachibana, K., and Kondo, T. (2006). Optimized ultrasound-mediated gene transfection in cancer cells. Cancer Sci. 97, 1111–1114.

Figueiredo, M.L., Kim, Y., St. John, M.A., and Wong, D.T. (2005). p12CDK2-AP1 gene therapy strategy inhibits tumor growth in an *in vivo* mouse model of head and neck cancer. Clin. Cancer Res. 11, 3939–3948.

Fitzgerald, D.C., Zhang, G.X., El-Behi, M., *et al.* (2007). Suppression of autoimmune inflammation of the central nervous system by interleukin 10 secreted by interleukin 27-stimulated T cells. Nat. Immunol. 8, 1372–1379.

Freeman, S.M., Ramesh, R., and Marrogi, A.J. (1997). Immune system in suicide-gene therapy. Lancet 349, 2–3.

Fujita, T., Teh, B.S., Timme, T.L., *et al.* (2006). Sustained long-term immune responses after in situ gene therapy combined with radiotherapy and hormonal therapy in prostate cancer patients. Int. J. Radiat. Oncol. Biol. Phys. 65, 84–90.

Gallina, G., Dolcetti, L., Serafini, P., *et al.* (2006). Tumors induce a subset of inflammatory monocytes with immunosuppressive activity on CD8+ T cells. J. Clin. Invest. 116, 2777–2790.

Ghiringhelli, F., Ménard, C., Terme, M., *et al.* (2005). $CD4^+$ $CD25^+$ regulatory T cells inhibit natural killer cell functions in a transforming growth factor-β-dependent manner. J. Exp. Med. 202, 1075–1085.

Hauff, P., Seemann, S., Reszka, R., *et al.* (2005). Evaluation of gas-filled microparticles and sonoporation as gene delivery system: feasibility study in rodent tumor models. Radiology 236, 572–578.

Huber, M., Steinwald, V., Guralnik, A., *et al.* (2008). IL-27 inhibits the development of regulatory T cells via STAT3. Int. Immunol. 20, 223–234.

Hwang, K.S., Cho, W.K., Yoo, J., *et al.* (2005). Adenovirus-mediated interleukin-12 gene transfer combined with cytosine deaminase followed by 5-fluorocytosine treatment exerts potent antitumor activity in Renca tumor-bearing mice. BMC Cancer 5, 51.

Lentacker, I., De Smedt, S.C., and Sanders, N.N. (2009). Drug loaded microbubble design for ultrasound triggered delivery. Soft Matter 5, 2161–2170.

Li, Y.S., Davidson, E., Reid, C.N., and McHale, A.P. (2009). Optimising ultrasound-mediated gene transfer (sonoporation) *in vitro* and prolonged expression of a transgene *in vivo*: potential applications for gene therapy of cancer. Cancer Lett. 273, 62–69.

Lucas, S., Ghilardi, N., Li, J., and de Sauvage, F.J. (2003). IL-27 regulates IL-12 responsiveness of naïve $CD4^+$ T cells through Stat1-dependent and -independent mechanisms. Proc. Natl. Acad. Sci. U.S.A. 100, 15047–15052.

Nakamori, M., Iwahashi, M., Ueda, K., *et al.* (2002). Dose of adenoviral vectors expressing interleukin-2 plays an important role in combined gene therapy with cytosine deaminase/5-fluorocytosine: preclinical consideration. Jpn. J. Cancer Res. 93, 706–715.

Neufert, C., Becker, C., Wirtz, S., *et al.* (2007). IL-27 controls the development of inducible regulatory T cells and Th17 cells via differential effects on STAT1. Eur. J. Immunol. 37, 1809–1816.

Newman, C.M., and Bettinger, T. (2007). Gene therapy progress and prospects: ultrasound for gene transfer. Gene Ther. 14, 465–475.

Passineau, M.J., Zourelias, L., Machen, L., *et al.* (2010). Ultrasound-assisted non-viral gene transfer to the salivary glands. Gene Ther. 17, 1318–1324; erratum 18, 424.

Pflanz, S., Timans, J.C., Cheung, J., *et al.* (2002). IL-27, a heterodimeric cytokine composed of EBI3 and p28 protein, induces proliferation of naive $CD4^+$ T cells. Immunity 16, 779–790.

Phillips, L.C., Klibanov, A.L., Wamhoff, B.R., and Hossack, J.A. (2010). Targeted gene transfection from microbubbles into vascular smooth muscle cells using focused, ultrasound-mediated delivery. Ultrasound Med. Biol. 36, 1470–1480.

Pislaru, S.V., Pislaru, C., Kinnick, R.R., *et al.* (2003). Optimization of ultrasound-mediated gene transfer: comparison of contrast agents and ultrasound modalities. Eur. Heart J. 24, 1690–1698.

Sakakima, Y., Hayashi, S., Yagi, Y., *et al.* (2005). Gene therapy for hepatocellular carcinoma using sonoporation enhanced by contrast agents. Cancer Gene Ther. 12, 884–889.

Salcedo, R., Stauffer, J.K., Lincoln, E., *et al.* (2004). IL-27 mediates complete regression of orthotopic primary and metastatic murine neuroblastoma tumors: role for $CD8^+$ T cells. J. Immunol. 173, 7170–7182.

Stride, E.P., and Coussios, C.C. (2010). Cavitation and contrast: the use of bubbles in ultrasound imaging and therapy. Proc. Inst. Mech. Eng. H. 224, 171–191.

Suzuki, R., Oda, Y., Namai, E., *et al.* (2008). [Development of site specific gene delivery system with sonoporation]. Yakugaku Zasshi 128, 187–192.

Suzuki, R., Namai, E., Oda, Y., *et al.* (2010). Cancer gene therapy by IL-12 gene delivery using liposomal bubbles and tumoral ultrasound exposure. J. Control. Release. 142, 245–250.

Takeda, A., Hamano, S., Yamanaka, A., *et al.* (2003). Cutting edge: role of IL-27/WSX-1 signaling for induction of T-bet through activation of STAT1 during initial Th1 commitment. J. Immunol. 170, 4886–4890.

Thompson, T.C., Southgate, J., Kitchener, G., and Land, H. (1989). Multistage carcinogenesis induced by *ras* and *myc* oncogenes in a reconstituted organ. Cell 56, 917–930.

Toda, M., Martuza, R.L., and Rabkin, S.D. (2001). Combination suicide/cytokine gene therapy as adjuvants to a defective herpes simplex virus-based cancer vaccine. Gene Ther. 8, 332–339.

Tsai, K.C., Liao, Z.K., Yang, S.J., *et al.* (2009). Differences in gene expression between sonoporation in tumor and in muscle. J. Gene Med. 11, 933–940.

Wells, D.J. (2010). Electroporation and ultrasound enhanced non-viral gene delivery in vitro and in vivo. Cell Biol. Toxicol. 26, 21–28.

Wu, Z., McRoberts, K.S., and Theodorescu, D. (2007). The role of PTEN in prostate cancer cell tropism to the bone microenvironment. Carcinogenesis 28, 1393–1400.

Zhu, S., Lee, D.A., and Li, S. (2010). IL-12 and IL-27 sequential gene therapy via intramuscular electroporation delivery for eliminating distal aggressive tumors. J. Immunol. 184, 2348–2354.

Zolochevska, O., and Figueiredo, M.L. (2011). Cell-cycle regulators cdk2ap1 and bicalutamide suppress malignant biological interactions between prostate cancer and bone cells. Prostate 71, 353–367.

Address correspondence to:
Dr. Marxa L. Figueiredo
University of Texas Medical Branch
Department of Pharmacology & Toxicology
301 University Blvd., MRB 7.102C
Galveston, TX 77555

E-mail: mlfiguei@utmb.edu

Received for publication May 5, 2011;
accepted after revision July 29, 2011.

Published online: July 29, 2011.